JACS
JOURNAL OF THE AMERICAN CHEMICAL SOCIETY
Communication
pubs.acs.org/JACS
Open Access on 08/12/2015

Spectroscopic Characterization and Reactivity Studies of a Mononuclear Nonheme Mn(III)−Hydroperoxo Complex

Hee So,[†,⊥] Young Jun Park,[†,⊥] Kyung-Bin Cho,[†] Yong-Min Lee,[†] Mi Sook Seo,[†] Jaeheung Cho,[‡] Ritimukta Sarangi,*[,§] and Wonwoo Nam*[,†]

[†]Department of Chemistry and Nano Science, Ewha Womans University, Seoul 120-750, Korea

[‡]Department of Emerging Materials Science, DGIST, Daegu 711-873, Korea

[§]Stanford Synchrotron Radiation Lightsource, SLAC National Accelerator Laboratory, Stanford University, Menlo Park, California 94025-7015, United States

Supporting Information

ABSTRACT: We report the first example of a mononuclear nonheme manganese(III)−hydroperoxo complex derived from protonation of an isolated manganese(III)−peroxo complex bearing an *N*-tetramethylated cyclam (TMC) ligand, $[Mn^{III}(TMC)(OOH)]^{2+}$. The Mn^{III}-hydroperoxo intermediate is characterized with various spectroscopic methods as well as with density functional theory (DFT) calculations, showing the binding of a hydroperoxide ligand in an end-on fashion. The Mn^{III}−hydroperoxo species is a competent oxidant in oxygen atom transfer (OAT) reactions, such as the oxidation of sulfides. The electrophilic character of the Mn^{III}−hydroperoxo complex is demonstrated unambiguously in the sulfoxidation of *para*-substituted thioanisoles.

Manganese(III)−peroxo (Mn^{III}−O_2) and manganese(III)−hydroperoxo (Mn^{III}−OOH) species have been invoked as key intermediates in the activation and formation of dioxygen (O_2) and the detoxification of reactive oxygen species by enzymes and their biomimetic compounds.[1,2] For example, manganese superoxide dismutase (Mn-SOD) catalyzes the disproportionation of superoxide to dioxygen and hydrogen peroxide.[1] At higher superoxide concentrations, the activity of Mn-SOD diminishes owing to the formation of a product-inhibited complex; the structure of this intermediate has been proposed to be a side-on Mn^{III}−peroxo or an end-on Mn^{III}−hydroperoxo species.[3,4] In water oxidation by the oxygen evolving complex (OEC) in Photosystem II (PSII), the final short-lived state (S_4) accompanies an O−O bond forming event to generate a putative Mn^{III}−OO(H)−Ca^{II} species, although no structural or spectroscopic information on the key intermediate has been obtained to date.[2]

In biomimetic studies, the first crystal structure of a Mn^{III}−peroxo porphyrin complex was reported by Valentine et al. in 1987.[5a] Since then, a number of Mn^{III}−peroxo complexes bearing nonheme ligands have been characterized structurally and/or spectroscopically and their reactivities have been well demonstrated in nucleophilic reactions.[5−8] In addition to the Mn^{III}−peroxo species, Kovacs et al. reported very recently the first example of structurally characterized Mn^{III}−alkylperoxo species and their reactivities in the alkylperoxo O−O bond cleavage.[9] However, to the best of our knowledge, no clear spectroscopic and/or structural data for Mn^{III}−hydroperoxo species have been obtained yet in heme and nonheme systems.

Herein we report the first example of a mononuclear nonheme Mn^{III}−hydroperoxo species derived from protonation of an isolated Mn^{III}−peroxo complex bearing an *N*-tetramethylated cyclam (TMC) ligand (Scheme 1). Spectroscopic data, including electronic absorption (UV−vis), resonance Raman (rRaman), electron paramagnetic resonance (EPR), and X-ray absorption spectroscopy/extended X-ray absorption fine structure (XAS/EXAFS), of the Mn^{III}−hydroperoxo species are reported. The Mn^{III}−hydroperoxo complex shows high reactivity with electrophilic character in sulfoxidation reactions (Scheme 1).

Scheme 1

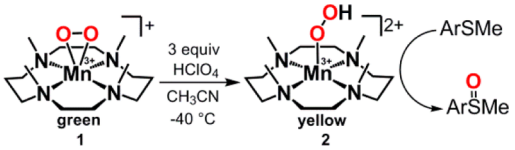

Addition of 3 equiv of $HClO_4$ to a solution of $[Mn^{III}(TMC)(O_2)]^+$ (**1**; TMC = 1,4,8,11-tetramethyl-1,4,8,11-tetraazacyclotetradecane) in CH_3CN at −40 °C under an Ar atmosphere resulted in formation of a yellow intermediate (**2**) with electronic absorption bands at λ_{max}/nm (ε_M/cm^{-1} M^{-1}) = 324 (6400) and 384 (8000) immediately (Figure 1a). **2** was highly stable at −40 °C under an Ar atmosphere ($t_{1/2}$ ∼1 day) but decayed at a fast rate at room temperature (rt). The intermediate **2** reverted back to **1** upon addition of 3 equiv of triethylamine (Supporting Information (SI), Figure S1), suggesting that **1** and **2** are interconvertible through reactions similar to the previously reported acid−base chemistry between nonheme iron(III)−peroxo and iron(III)−hydroperoxo species.[10] Attempts to isolate **2** as crystalline material were not successful; therefore, the intermediate **2** was characterized using various spectroscopic techniques, including rRaman, EPR, XAS/EXAFS, and DFT.

Received: June 23, 2014
Published: August 12, 2014

   dx.doi.org/10.1021/ja506275q | J. Am. Chem. Soc. 2014, 136, 12229−12232

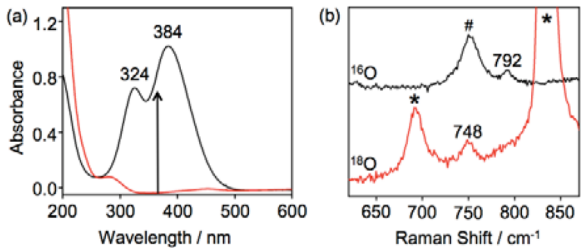

Figure 1. (a) UV−vis spectra of **1** (red line) and **2** (black line) in CH_3CN (0.13 mM) at −40 °C. (b) Resonance Raman spectra of **2** (black line) in CH_3CN and ^{18}O-labeled **2** (red line) in CD_3CN at −40 °C. # and * denote solvent peaks from CH_3CN and CD_3CN, respectively.

The rRaman spectrum of **2**, obtained upon 407 nm excitation in CH_3CN at −40 °C, exhibits an isotopically sensitive band at 792 cm^{-1} (Figure 1b). The peak shifted to 748 cm^{-1} when **2** was prepared with $[Mn^{III}(TMC)(^{18}O_2)]^+$ (**1**-^{18}O) (SI, Experimental Section). The observed shift of $^{16,18}\Delta$ = 44 cm^{-1} is in good agreement with the calculated value of 45 cm^{-1} for a harmonic O−O oscillator. The isotopically sensitive bands disappeared upon warming the samples to rt, indicating that these peaks are not derived from solvents. It is noteworthy that the O−O vibrational frequency of **2** (792 cm^{-1}) is lower than those for Mn^{III}−O_2 (~900 cm^{-1}) and Mn^{III}−O_2R (~880 cm^{-1})[6a,7a,8c,11] species, but falls in the range of the spectroscopically characterized mononuclear Fe^{III}−hydroperoxo species (780−840 cm^{-1}).[12] Similar to **1**,[7c] **2** was EPR silent.[13] The spin state of **2** was determined to be S = 2 (μ_{eff} = 5.1 μ_B) by ^1H NMR spectroscopic analysis using Evans' method.[14]

XAS analysis, including XANES and EXAFS, clearly supports the formulation of **2** as a $[Mn^{III}(TMC)(OOH)]^{2+}$ dication species. The normalized Mn K-edge XAS data for **1** and **2** are compared to those of $[Mn^{II}(TMC)]^{2+}$ in Figure 2. The data

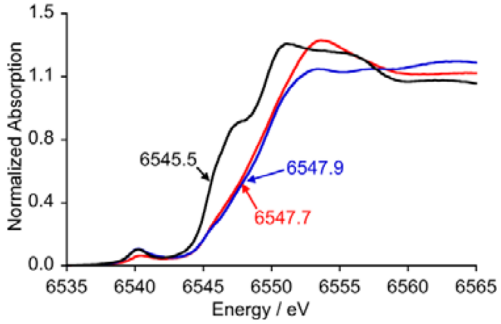

Figure 2. Normalized Mn K-edge XAS spectra for **1** (blue line) and **2** (red line) compared to the starting $[Mn^{II}(TMC)]^{2+}$ species (black line). The arrows point to the rising-edge at half maxima (0.5 normalized intensity).

show a shift in the rising-edge position of **1** and **2** to higher energy by over 2 eV (2.4 eV for **1** and 2.2 eV for **2**), clearly indicating that the oxidation states of both Mn ions in **1** and **2** are +3. The local structure of these two Mn^{III} species was investigated using EXAFS. A comparison of the EXAFS and Fourier transform data for **1** and **2** is shown in Figure 3a. The comparison shows that, on going from **1** to **2**, the intensity of the first shell peak drops significantly and is slightly shifted to a higher R' value. Redistribution of the outer shell single and multiple scattering is also observed, but the change is smaller compared to that in the first shell.

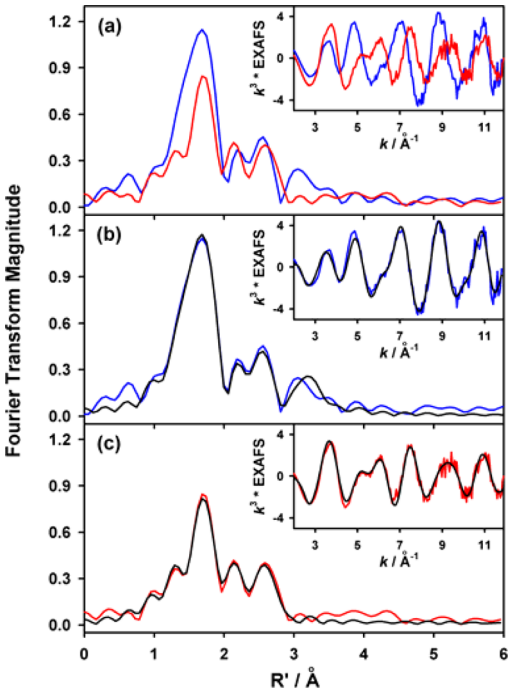

Figure 3. (a) A comparison of the non phase-shift corrected Fourier transforms and the corresponding Mn K-edge EXAFS data (inset) for **1** (blue line) and **2** (red line). FEFF best fits to **1** and **2** together with original data (blue and red lines) are shown in (b) and (c) as a black line, respectively. Fits were performed over k = 2−12 $Å^{-1}$ range.

FEFF fits to the non phase-shift corrected Fourier transform of **1** and the corresponding EXAFS data are shown in Figure 3b. Least-squares fit results show that the data are most consistent with a first shell composed of two Mn−O at 1.88 Å and four Mn−N components at 2.24 Å (SI, Table S2). The second and third shells are fit with single and multiple-scattering components from the TMC ligand. The number of independent parameters used for the fit was 11 (allowed independent parameters using Stern's rule: $2\delta k\delta r/\pi + 2 = 14$). Together, the edge and EXAFS data are consistent with a side-on bound Mn^{III}−O_2^{2-} description for **1**. The least-squares EXAFS fit results for **2** are presented in Figure 3c. In **2**, the first shell is fit with one Mn−O at 1.93 Å and four Mn−N at 2.17 Å. The outer shells are fit with single and multiple scattering contributions from the TMC ligand (SI, Table S2). These results reveal that **2** is an end-on bound Mn^{III}−OOH species.

DFT calculations were also performed on the peroxo monocation **1** (SI, Tables S3−S5) and hydroperoxo dication **2** (SI, Tables S6−S8) species in the S = 1 and 2 spin states. Total energy comparisons show that both **1** and **2** energetically prefer the S = 2 state by about 20 kcal/mol (SI, Tables S3 and S6). The structures with the four methyl groups *syn* to the $O_2(H)$ group(s) are preferred, as they are both energetically favorable and in good agreement with the EXAFS data (see SI, Tables S5 and S8). Numerical frequency calculations yielded an O−O stretching frequency of 934 and 857 cm^{-1} for **1** and **2**, respectively, which is in good agreement with the rRaman data indicating the weakening of the O−O bond upon protonation.

Since we have shown recently that a high-spin iron(III)−hydroperoxo complex, $[Fe^{III}(TMC)(OOH)]^{2+}$, is an active oxidant in both oxygen atom transfer (OAT) and hydrogen atom transfer (HAT) reactions,[15] we tested the manganese analog, **2**, in those reactions. Unlike the reactivity of the

dx.doi.org/10.1021/ja506275q | J. Am. Chem. Soc. 2014, 136, 12229−12232

$[Fe^{III}(TMC)(OOH)]^{2+}$ complex in HAT reactions, **2** did not react with cyclohexadiene in CH_3CN at −40 °C, indicating that **2** is not capable of activating C−H bonds. However, **2** disappeared immediately upon addition of 4-methoxythioanisole (40 equiv) in CH_3CN at −40 °C, suggesting its activity in OAT reaction. Therefore, the reactivity of **2** in sulfoxidation reactions was investigated using a stopped-flow spectrometer. The first-order rate constant (k_{obs}) was determined to be 1.6×10^2 s^{-1} at −40 °C in the reaction of 4-methoxythioanisole (Figure 4a), and the first-order rate constants increased

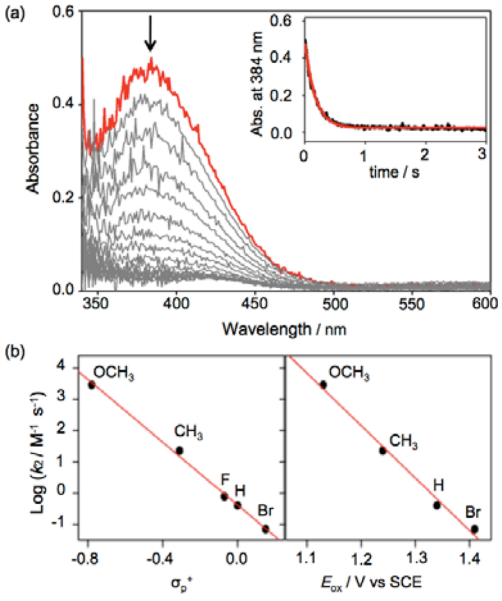

Figure 4. (a) UV−vis spectral changes, monitored by stopped-flow technique, showing the decay of $[Mn^{III}(TMC)(OOH)]^{2+}$ (**2**, 0.060 mM) upon mixing of 4-methoxythioanisole (40 equiv; 2.4 mM) in CH_3CN at −40 °C. Inset shows the time course of the absorbance change of **2** (black line) and the corresponding pseudo-first-order fit (red line) at 384 nm. (b) Hammett plot of log k_2 against σ_p^+ of *para*-X−Ph−SCH_3 (left panel) and plot of log k_2 against E_{ox} of *para*-X−Ph−SCH_3 (right panel).

proportionally with an increase of the substrate concentration to give a second-order rate constant (k_2) of 2.9×10^3 M^{-1} s^{-1} at −40 °C (SI, Figure S2a). The reactivity of **2** was further investigated with *para*-substituted thioanisoles, *para*-X−Ph−SCH_3 (X = OCH_3, CH_3, F, H, Br), to investigate the electronic effect of *para*-substituents on the oxidation of thioanisoles by **2** (Figure 4b). A Hammett plot of the second-order rate constants vs σ_p^+ gave a ρ value of −5.0 (Figure 4b, left panel; SI, Table S1), confirming the electrophilic character of the hydroperoxo group in **2**.[16] In addition, we observed a good linear correlation when the rates were plotted against oxidation potentials (E_{ox}) of thioanisoles (Figure 4b, right panel; SI, Table S1). The negative slope of −17 for **2** is significantly larger than that obtained in the sulfoxidation reaction by Fe^{III}−hydroperoxo (slope = −2.5).[15c] Based on the previous reports in high-valent metal−oxo species,[16] we propose that the oxidation of sulfides by **2** proceeds via electron transfer, followed by oxygen atom transfer, although **2** is a metal−hydroperoxo species.

Organic product analysis of the reaction solution by HPLC revealed that methyl phenyl sulfoxide was produced in good yield (>60% based on the amount of **2** used). In addition, by analyzing the reaction solution with EPR and electrospray ionization mass spectrometry (ESI MS), we found that a Mn^{II} species was formed as a major product in the sulfoxidation reaction by **2** (SI, Figures S3 and S4). Although the exact mechanism of the formation of the Mn^{II} species is not clear, we propose that the Mn product formed in this reaction (e.g., $[(TMC)Mn^{III}(OH)]^{2+}$) is not stable and decomposes to the Mn^{II} species under reaction conditions, similar to that observed in the sulfoxidation reaction by Fe(III)−hydroperoxo species.[15c] DFT calculations have been performed for this reaction, modeled by a direct attack of **2** on a thioanisole substrate (SI, Tables S9−S11). The calculations show a heterolytic cleavage ($[Mn^{III}O]^+ + OH^+$) over a barrier of 16.5 kcal/mol, followed by S−OH bond formation and a simultaneous barrierless H^+ transfer back to form $[Mn^{III}OH]^{2+}$ (see SI, Figure S5). The heterolytic cleavage is shown by the Mulliken spin density distribution of 0.07 on the leaving OH^+ group (see SI, Table S10). This is analogous to the earlier reported Fe case, where it has been shown that a singly occupied π^*_{xz} orbital (as in **2**) renders a heterolytic cleavage.[15c] Detailed studies on the mechanism of the sulfoxidation by **2** and the reactivity comparison of **2** and $[Fe^{III}(TMC)(OOH)]^{2+}$ are underway in this laboratory.

In summary, we have reported the first clear spectroscopic and reactivity properties of a mononuclear nonheme Mn^{III}−hydroperoxo species. The Mn^{III}−hydroperoxo complex has been successfully generated by direct protonation of the parent Mn^{III}−peroxo species. The successive interconversion of hydroperoxo to peroxo by the addition of a base further supports their conjugated acid−base nature. The most striking outcomes from this simple protonation reaction of Mn^{III}−peroxo species are as follows: First, the electronic transition is significantly perturbed (showing a color change from green to yellow).[17] This optical change will be further investigated by using spectroscopic and computational methods to understand the general property of the mononuclear Mn^{III}−hydroperoxo system in detail. Second, unlike the Mn^{III}−peroxo in **1**, the Mn^{III}−hydroperoxo in **2** performs an electrophilic sulfoxidation reaction, which might be the consequence of electronic regulation by the proton as a Lewis acid. It has been reported recently that metal−oxidant adducts (M^{n+}−OX where X = IAr, OH, OR, and halides) are capable of oxidizing substrates prior to the O−X bond cleavage to form their high-valent metal−oxo species.[18] With the Mn^{III}−peroxo (**1**) and Mn^{III}−hydroperoxo (**2**) complexes bearing a common supporting ligand, our future studies will focus on the structural and spectroscopic comparison as well as the reactivity comparison in substrate oxidation and electron transfer reactions, which may provide clues to understand the structures and functional roles of the proposed Mn^{III}−peroxo and Mn^{III}−hydroperoxo intermediates in the reactions of nonheme Mn-containing enzymes.[1−4]

■ ASSOCIATED CONTENT

Supporting Information

Experimental details for all chemical reactions and measurements, figures for optical and EPR spectra, and details on theoretical calculations. This material is available free of charge via the Internet at http://pubs.acs.org.

■ AUTHOR INFORMATION

Corresponding Authors

wwnam@ewha.ac.kr
ritis@slac.stanford.edu

Author Contributions

[⊥]H.S. and Y.J.P. contributed equally to this work.

Notes

The authors declare no competing financial interest.

■ ACKNOWLEDGMENTS

The authors gratefully acknowledge research support of this work by the NRF of Korea MSIP through CRI (NRF-2012R1A3A2048842 to W.N.), GRL (NRF-2010-00353 to W.N.), Research Fellow program (2013R1A1A2061528 to Y.J.P. and 2013R1A1A2062737 to K.-B.C.), and the R&D programs (14-BD-0403 and 2013K2A2A4000610 to J.C.) and KCRC (NRF-2014M1A8A1049320) of the Ministry of Science, ICT & Future Planning of Korea. Use of the Stanford Synchrotron Radiation Lightsource, SLAC National Accelerator Laboratory, is supported by the U.S. Department of Energy, Office of Science, Office of Basic Energy Sciences under Contract No. DE-AC02-76SF00515. The SSRL Structural Molecular Biology Program is supported by the DOE Office of Biological and Environmental Research and by the National Institutes of Health, National Institute of General Medical Sciences (including P41GM103393).

■ REFERENCES

(1) (a) Sheng, Y.; Abreu, I. A.; Cabelli, D. E.; Maroney, M. J.; Miller, A.-F.; Teixeira, M.; Valentine, J. S. *Chem. Rev.* **2014**, *114*, 3854. (b) Grove, L. E.; Brunold, T. C. *Comments Inorg. Chem.* **2008**, *29*, 134. (c) Wu, A. J.; Penner-Hahn, J. E.; Pecoraro, V. L. *Chem. Rev.* **2004**, *104*, 903.

(2) (a) McEvoy, J. P.; Brudvig, G. W. *Chem. Rev.* **2006**, *106*, 4455. (b) Nocera, D. G. *Acc. Chem. Res.* **2012**, *45*, 767. (c) Cox, N.; Pantazis, D. A.; Neese, F.; Lubits, W. *Acc. Chem. Res.* **2013**, *46*, 1588.

(3) (a) Bull, C.; Niederhoffer, E. C.; Yoshida, T.; Fee, J. A. *J. Am. Chem. Soc.* **1991**, *113*, 4069. (b) Hearn, A. S.; Tu, C. K.; Nick, H. S.; Silverman, D. N. *J. Biol. Chem.* **1999**, *274*, 24457. (c) Jackson, T. A.; Karapetian, A.; Miller, A.-F.; Brunold, T. C. *Biochemistry* **2005**, *44*, 1504. (d) Abreu, I. A.; Rodriguez, J. A.; Cabelli, D. E. *J. Phys. Chem. B* **2005**, *109*, 24502.

(4) For an X-ray structure of the peroxide-soaked MnSOD crystal, see: Porta, J.; Vahedi-Faridi, A.; Borgstahl, G. E. O. *J. Mol. Biol.* **2010**, *399*, 377.

(5) (a) VanAtta, R. B.; Strouse, C. E.; Hanson, L. K.; Valentine, J. S. *J. Am. Chem. Soc.* **1987**, *109*, 1425. (b) Wertz, D. L.; Valentine, J. S. *Struct. Bonding (Berlin)* **2000**, *97*, 37.

(6) (a) Leto, D. F.; Jackson, T. A. *J. Biol. Inorg. Chem.* **2014**, *19*, 1. (b) Cho, J.; Sarangi, R.; Nam, W. *Acc. Chem. Soc.* **2012**, *45*, 1321.

(7) (a) Kitajima, N.; Komatsuzaki, H.; Hikichi, S.; Osawa, M.; Moro-oka, Y. *J. Am. Chem. Soc.* **1994**, *116*, 11596. (b) Singh, U. P.; Sharma, A. K.; Hikichi, S.; Komatsuzaki, H.; Moro-oka, Y.; Akita, M. *Inorg. Chim. Acta* **2006**, *359*, 4407. (c) Seo, M. S.; Kim, J. Y.; Annaraj, J.; Kim, Y.; Lee, Y.-M.; Kim, S.-J.; Kim, J.; Nam, W. *Angew. Chem., Int. Ed.* **2007**, *46*, 377. (d) Annaraj, J.; Cho, J.; Lee, Y.-M.; Kim, S. Y.; Latifi, R.; de Visser, S. P.; Nam, W. *Angew. Chem., Int. Ed.* **2009**, *48*, 4150. (e) Kang, H.; Cho, J.; Cho, K.-B.; Nomura, T.; Ogura, T.; Nam, W. *Chem.—Eur. J.* **2013**, *19*, 14119.

(8) (a) Groni, S.; Blain, G.; Guillot, R.; Policar, C.; Anxolabéhère-Mallart, E. *Inorg. Chem.* **2007**, *46*, 1951. (b) Groni, S.; Dorlet, P.; Blain, G.; Bourcier, S.; Guillot, R.; Anxolabéhère-Mallart, E. *Inorg. Chem.* **2008**, *47*, 3166. (c) Shook, R. L.; Gunderson, W. A.; Greaves, J.; Ziller, J. W.; Hendrich, M. P.; Borovik, A. S. *J. Am. Chem. Soc.* **2008**, *130*, 8888. (d) Geiger, R. A.; Chattopadhyay, S.; Day, V. W.; Jackson, T. A. *J. Am. Chem. Soc.* **2010**, *132*, 2821. (e) Shook, R. L.; Peterson, S. M.; Greaves, J.; Moore, C.; Rheingold, A. L.; Borovik, A. S. *J. Am. Chem. Soc.* **2011**, *133*, 5810. (f) Geiger, R. A.; Leto, D. F.; Chattopadhyay, S.; Dorlet, P.; Anxolabéhère-Mallart, E.; Jackson, T. A. *Inorg. Chem.* **2011**, *50*, 10190. (g) Ghachtouli, S. E.; Ching, H. Y. V.; Lassalle-Kaiser, B.; Guillot, R.; Leto, D. F.; Chattopadhyay, S.; Jackson, T. A.; Dorlet, P.; Anxolabéhère-Mallart, E. *Chem. Commun.* **2013**, *49*, 5696.

(9) (a) Coggins, M. K.; Kovacs, J. A. *J. Am. Chem. Soc.* **2011**, *133*, 12470. (b) Coggins, M. K.; Martin-Diaconescu, V.; DeBeer, S.; Kovacs, J. A. *J. Am. Chem. Soc.* **2013**, *135*, 4260.

(10) (a) Jensen, K. B.; McKenzie, C. J.; Nielsen, P. L.; Pedersen, J. Z.; Svendsen, H. M. *Chem. Commun.* **1999**, 1313. (b) Neese, F.; Solomon, E. I. *J. Am. Chem. Soc.* **1998**, *120*, 12829.

(11) Coggins, M. K.; Sun, X.; Kwak, Y.; Solomon, E. I.; Rybak-Akimova, E.; Kovacs, J. A. *J. Am. Chem. Soc.* **2013**, *135*, 5631.

(12) (a) Girerd, J.-J.; Banse, F.; Simaan, A. J. *Struct. Bonding (Berlin)* **2000**, *97*, 145. (b) Roelfes, G.; Vrajmasu, V.; Chen, K.; Ho, R. Y. N.; Rohde, J.-U.; Zondervan, C.; Crois, R. M.; Schudde, E. P.; Lutz, M.; Spek, A. L.; Hage, R.; Feringa, B. L.; Munck, E.; Que, L., Jr. *Inorg. Chem.* **2003**, *42*, 2639.

(13) An isotropic six-line signal around $g = 2$ from small amounts of Mn^{II} impurity was also observed.

(14) (a) Evans, D. F. *J. Chem. Soc.* **1959**, 2003. (b) Evans, D. F.; Jakubovic, D. A. *J. Chem. Soc., Dalton Trans.* **1988**, 2927.

(15) (a) Cho, J.; Jeon, S.; Wilson, S. A.; Liu, L. V.; Kang, E. A.; Braymer, J. J.; Lim, M. H.; Hedman, B.; Hodgson, K. O.; Valentine, J. S.; Solomon, E. I.; Nam, W. *Nature* **2011**, *478*, 502. (b) Liu, L. V.; Hong, S.; Cho, J.; Nam, W.; Solomon, E. I. *J. Am. Chem. Soc.* **2013**, *135*, 3286. (c) Kim, Y. M.; Cho, K.-B.; Cho, J.; Wang, B.; Li, C.; Shaik, S.; Nam, W. *J. Am. Chem. Soc.* **2013**, *135*, 8838.

(16) (a) Goto, Y.; Matsui, T.; Ozaki, S.; Watanabe, Y.; Fukuzumi, S. *J. Am. Chem. Soc.* **1999**, *121*, 9497. (b) Arias, J.; Newlands, C. R.; Abu-Omar, M. M. *Inorg. Chem.* **2001**, *40*, 2185. (c) Taki, M.; Itoh, S.; Fukuzumi, S. *J. Am. Chem. Soc.* **2002**, *124*, 998. (d) McPherson, L. D.; Drees, M.; Khan, S. I.; Strassner, T.; Abu-Omar, M. M. *Inorg. Chem.* **2004**, *43*, 4036. (e) Bang, S.; Park, S.; Lee, Y.-M.; Hong, S.; Cho, K.-B.; Nam, W. *Angew. Chem., Int. Ed.* **2014**, *53*, 7843.

(17) The observed spectral change is markedly different from the similar attempts by Groni et al. using $[Mn^{III}(MeTPEN)(O_2)]^+$ (MeTPEN = *N*-methyl-*N*,*N*′,*N*′-tris(2-pyridylmethyl)ethane-1,2-diamine) and the same acid (e.g., perchloric acid); see ref 8a and b.

(18) (a) Wang, C.; Kurahashi, T.; Fujii, H. *Angew. Chem., Int. Ed.* **2012**, *51*, 7809. (b) Cong, Z.; Yanagisawa, S.; Kurahashi, T.; Ogura, T.; Nakashima, S.; Fujii, H. *J. Am. Chem. Soc.* **2012**, *134*, 20617. (c) Guo, M.; Dong, H.; Li, J.; Cheng, B.; Huang, Y.-q.; Feng, Y.-q.; Lei, A. *Nat. Commun.* **2012**, *3*, 1190. (d) Wang, C.; Kurahashi, T.; Inomata, K.; Hada, M.; Fujii, H. *Inorg. Chem.* **2013**, *52*, 9357. (e) Hong, S.; Wang, B.; Seo, M. S.; Lee, Y.-M.; Kim, H. R.; Ogura, T.; Garcia-Serres, R.; Clémancey, M.; Latour, J.-M.; Nam, W. *Angew. Chem., Int. Ed.* **2014**, *53*, 6388.